

# InAs Photodiodes for 3.43 $\mu\text{m}$ Radiation Thermometry

Xinxin Zhou, Xiao Meng, Andrey B. Krysa, Jon R. Willmott,  
Jo Shien Ng, *Member, IEEE*, and Chee Hing Tan, *Member, IEEE*

**Abstract**—We report an evaluation of an epitaxially grown uncooled InAs photodiode for the use in radiation thermometry. Radiation thermometry measurements was taken using the photodiode covered blackbody temperatures of 50 °C–300 °C. By determining the photocurrent and signal-to-noise ratio, the temperature error of the measurements was deduced. It was found that an uncooled InAs photodiode, with the peak and cutoff wavelengths of 3.35 and 3.55  $\mu\text{m}$ , respectively, measured a temperature of 50 °C, with an error of 0.17 °C. Many plastics have C–H molecular bond absorptions at 3.43  $\mu\text{m}$  and hence radiate thermally at this wavelength. Our results suggest that InAs photodiodes are well suited to measure the temperature of plastics above 50 °C. When tested with a narrow bandpass filter at 3.43  $\mu\text{m}$  and blackbody temperatures from 50 °C–300 °C, the InAs photodiode was also found to produce a higher output photocurrent, compared with a commercial PbSe detectors.

**Index Terms**—Radiation thermometry, temperature measurement, InAs photodiodes.

## I. INTRODUCTION

**R**ADIATION thermometers are used to monitor the temperature of an object without physical contact. The object's temperature is deduced from the measurement of the emitted energy from the object over a specific wavelength range [1]. These non-contact instruments are widely used in temperature measurements of plastics [2], glass [3] and metals [4]. Depending on their principles of operation, detectors used in radiation thermometers can be classed into one of two categories, thermal detectors and photon detectors. Thermal detectors include thermopiles, pyroelectric detectors and bolometers, all of which can respond to radiation over a broad wavelength spectrum and hence can detect down to ambient temperature or lower [5]. These thermal detectors produce changes in physical parameters that are proportional to the temperature of the object. Appropriate absorbent coatings on these detectors enable them to work as either a broad band or a narrow band thermometer. However, when operated

Manuscript received April 24, 2015; accepted June 7, 2015. Date of publication June 11, 2015; date of current version August 12, 2015. This work was supported in part by the European Space Agency under Contract 4000107110/12/NL/CBI and in part by the U.K. Engineering and Physical Sciences Research Council under Grant EP/H031464/1, Grant EP/I010920/1, and Grant EP/K001469/1. The associate editor coordinating the review of this paper and approving it for publication was Dr. M. N. Abedin.

The authors are with the Department of Electronic and Electrical Engineering, The University of Sheffield, Sheffield S1 3JD, U.K. (e-mail: x.zhou@sheffield.ac.uk; elp11xm@sheffield.ac.uk; a.krysa@sheffield.ac.uk; j.r.willmott@sheffield.ac.uk; j.s.ng@sheffield.ac.uk; c.h.tan@shef.ac.uk).

Color versions of one or more of the figures in this paper are available online at <http://ieeexplore.ieee.org>.

Digital Object Identifier 10.1109/JSEN.2015.2443563

without cooling, they suffer from long response time and low sensitivity, in comparison to photon detectors. A given photon detector is typically sensitive to photons within a narrower wavelength range [4]. Therefore semiconductors with different band gaps are normally employed to produce different photon detectors and these can be optimized to cover different applications and different temperature ranges.

A blackbody is a theoretical object that emits radiation with 100% efficiency. In practical temperature measurements, the emissivity factor, which is the ratio of spectral radiance from an object to that of a blackbody at the same temperature, must be known, in order for an accurate temperature measurement to be made. Uncertainty in the emissivity factor can lead to significant measurement error in radiation thermometry. Fortunately, at shorter wavelengths, such as 1–3  $\mu\text{m}$ , the spectral radiance changes with temperature more rapidly, compared to that at longer wavelengths, thus a smaller temperature error can be achieved by detecting the photons at shorter wavelengths [6]. In addition to the smaller error, short wavelength photon detectors have lower leakage current and hence lower shot noise, compared to long wavelength photon detectors. However, at temperatures below 1000 °C, significantly more power is radiated from a body at long wavelengths than short wavelengths. These define the design trade-offs between photo-generated signal and dark current in semiconductor photon detector.

Si and  $\text{In}_{0.47}\text{Ga}_{0.53}\text{As}$  (hereafter referred to as standard InGaAs) photodiodes are currently widely used in radiation thermometry [5], [7]. Due to the non-linear spectral power of Planck's law, these detectors' cut-off wavelengths of 1.0 and 1.6  $\mu\text{m}$  limit the minimum temperature that can be measured to 400 [5] and 150 °C [7] respectively. As the object temperature decreases, the peak in spectral radiance shifts to longer wavelengths, necessitating the use of narrower bandgap semiconductors to achieve longer cut-off wavelengths. For example by increasing the Indium (In) composition, extended InGaAs photodiodes detecting up to 2.6  $\mu\text{m}$  are commercially available. This enables commercial thermometers to detect temperatures down to 50 °C [8]. Lead salt detectors, such as PbS and PbSe photoconductors, with cut-off wavelengths at 3 and 5  $\mu\text{m}$  respectively, are also widely used in commercial thermometers to detect objects close to ambient temperature [9]. The uncooled photon detectors discussed above are summarized in table I.

The wavelength range of 3.0 - 3.65  $\mu\text{m}$  is of particular interest to narrow band radiation thermometry used for measuring temperatures of gases and certain plastics [10]. For instance, narrow band thermometers operating at 3.43  $\mu\text{m}$  are widely

TABLE I  
COMMON UNCOOLED PHOTON DETECTORS  
IN RADIATION THERMOMETERS

Detectors	Cut-off wavelength	Typical measurement range
Si	1.0 $\mu\text{m}$	400 - 2000 $^{\circ}\text{C}$ [5]
Standard InGaAs	1.6 $\mu\text{m}$	150 - 1000 $^{\circ}\text{C}$ [7]
Extended InGaAs	2.3 $\mu\text{m}$	50 - 400 $^{\circ}\text{C}$ [8]
PbS	3.0 $\mu\text{m}$	80 - 250 $^{\circ}\text{C}$ [9]
PbSe	5 $\mu\text{m}$	30 - 300 $^{\circ}\text{C}$ [9]

used in the processing of thin film plastics [11], [12], which have C-H bonds that resonate at this wavelength. As shown in table I, PbSe photoconductor is the only candidate for this operation wavelength range. The commercial thermometer using PbSe shows an accuracy rating of  $\pm 2$   $^{\circ}\text{C}$  under 200  $^{\circ}\text{C}$  ( $\pm 1\%$  of measured value at higher temperature) [9]. With a bandgap of 0.36 eV, InAs exhibits a cut-off wavelength of 3.55  $\mu\text{m}$  at room temperature, providing high sensitivity at the wavelengths range of 3.0 - 3.65  $\mu\text{m}$ . InAs photodiodes are, however, absent in the current portfolio of commercial uncooled radiation thermometers. Since an InAs photodiode can easily detect radiation at 3.43  $\mu\text{m}$ , in this work we performed detailed characterization of an epitaxially grown InAs photodiode and evaluated its potential for radiation thermometry.

## II. DEVICE STRUCTURE AND EXPERIMENTAL DETAILS

For a photodiode to achieve high responsivity, a wide depletion region in the structure is desirable. This in turn requires low unintentional doping in the photodiode's photon absorption layer. Using an epitaxially grown structure, an InAs photodiode with unintentional doping as low as  $7 \times 10^{14} \text{ cm}^{-3}$  was achieved in our laboratory [13]. The InAs wafer studied in this work was grown by metalorganic vapour phase epitaxy on a 2" p-type InAs substrate. The wafer structure consisted of a 2  $\mu\text{m}$  p<sup>+</sup> layer (doped with Zn at nominal concentration of  $1 \times 10^{18} \text{ cm}^{-3}$ ) followed by an 8  $\mu\text{m}$  intrinsic layer, and finally a 2  $\mu\text{m}$  n<sup>+</sup> layer (doped with Si at nominal concentration of  $1 \times 10^{18} \text{ cm}^{-3}$ ), as shown in Fig. 1(a). Mesa diodes with diameters of 420, 220, 120 and 70  $\mu\text{m}$ , also shown in Fig. 1(a), were fabricated from the wafer using wet chemical etchants [14] of phosphoric acid: hydrogen peroxide: deionized water (ratio of 1:1:1), followed by a finishing etch using sulphuric acid: hydrogen peroxide: de-ionized water (1:8:80). Ti/Au metal (20/200 nm thick) was deposited to form top and bottom ohmic contacts. No anti-reflection coating and passivation were added to these devices.

Current-Voltage (I-V) measurements of the photodiodes were performed using a Keithley 236 source-measurement unit. Spectral response measurements were performed using a Varian Fourier Transform infrared (FTIR) spectrometer. The responsivity was deduced using the normalized spectral response obtained from the FTIR and the peak responsivity measured using a blackbody temperature of 800  $^{\circ}\text{C}$ . Responsivity values at wavelengths of 0.633, 1.52 and 2.004  $\mu\text{m}$  were cross-checked with separate measurements using lasers at the respective wavelengths, as the photon source. For radiation

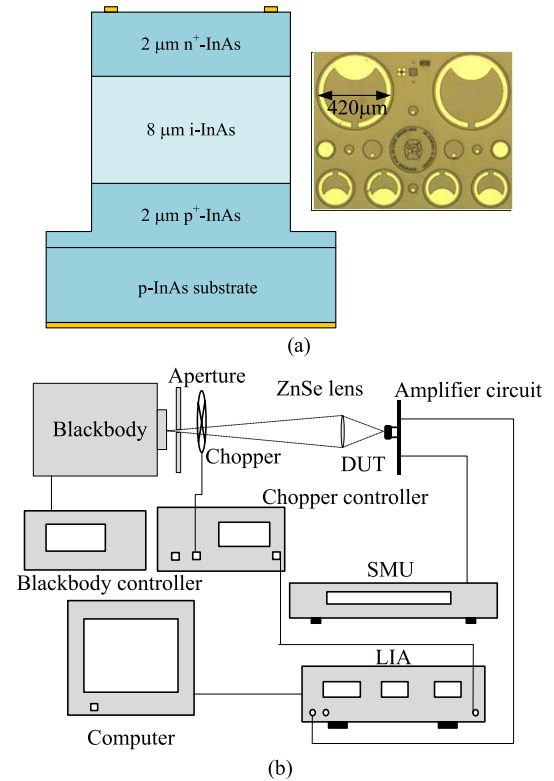


Fig. 1. (a) Cross sectional and top view of InAs diode. (b) Radiation thermometry measurement setup.

thermometry measurement the setup [15] shown schematically in Fig. 1(b) was used. A blackbody source, IR-563/301, with an aperture diameter of 7.5 mm was used. The radiated signal from the blackbody was modulated by a mechanical chopper at a frequency of 420 Hz, before being focused by a ZnSe lens (25.4 mm diameter plano-convex lenses, 50 mm focal length) onto the device under test (DUT). The DUT was placed at 300 mm from the blackbody source. The photocurrent from the DUT was amplified by in-house trans-impedance amplifier (TIA) circuit with an overall gain of  $10^6$  and noise of 125 nV/Hz<sup>1/2</sup> (obtained through separate measurements using an FFT spectrum analyzer). The output signal from the TIA, measured using the phase sensitive detection method by a SR830 lock-in amplifier, was used to deduce the photocurrent from the DUT. The largest device with 420  $\mu\text{m}$  diameter had a 60% fill factor, defined by the metal contact shown in Fig. 1(a). This was used for thermometry measurement in this work.

In order to deduce the temperature error,  $\Delta T$ , for a given set of conditions, we used 6 sets of data, with each set taken over a duration of 120 s using a sampling time of 0.05 s, giving a total duration of 720 s. Mean and standard deviation values,  $\langle I_{ph} \rangle$  and  $\sigma(I_{ph})$ , were then calculated for these data to yield the signal to noise ratio (SNR), defined as the ratio of  $\langle I_{ph} \rangle$  to  $\sigma(I_{ph})$ . The percentage error of the output,  $\%_{output\ error}$ , is related to SNR and is expressed as

$$\%_{output\ error} = 100 \times \frac{\sigma(I_{ph})}{\langle I_{ph} \rangle}.$$

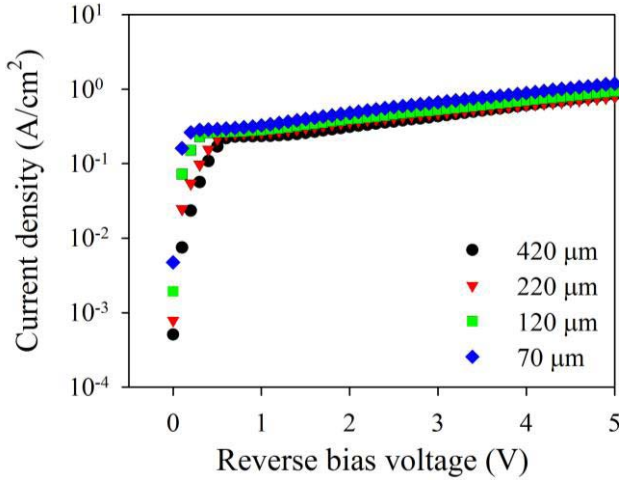


Fig. 2. Comparison of room temperature dark current density from InAs photodiodes with diameters ranging from 70 to 420  $\mu\text{m}$ .

The theoretical sensitivity of the system can be characterized by Percent-per-Degree, which is given by [16]  $\%/\text{°C} = 100 \times \frac{c_2}{\lambda T^2}$ , where  $c_2$  is Planck's second constant (1.4388  $\text{cm} \cdot \text{K}$ ),  $\lambda$  is the effective operational wavelength of the thermometer, and  $T$  is the object temperature in Kelvin. The effective wavelength is derived from the gradient of the natural logarithm of output photocurrent plotted as a function of  $1/T$  [17], [18]. This method is based on the Wien's law approximation to Planck's Law and is useful to model broad band radiations as a single monochromatic wavelength [19]. Finally the temperature error,  $\Delta T$ , is given by the ratio of  $\%_{\text{output error}}$  to  $\%/\text{°C}$ , and is expressed as

$$\Delta T = \frac{\sigma(I_{ph}) / \langle I_{ph} \rangle}{c_2 / \lambda T^2}.$$

### III. RESULTS AND DISCUSSION

Dark current densities measured from the InAs diodes with different diameters are in agreement, as shown in Fig. 2. Since the dark current due to bulk mechanisms scales with the diode area, an agreement of dark current densities indicates that bulk dark current dominates at room temperature, despite the absence of surface passivation in these diodes.

Fig. 3(a) compares the room temperature responsivity versus wavelength characteristics of our InAs photodiode at 0 and 0.1 V. With zero external bias, our InAs diode shows a peak responsivity of 1.28 A/W at 3.35  $\mu\text{m}$  and a cut-off wavelength (at 50 % of peak response) of 3.55  $\mu\text{m}$ , giving 48 % external quantum efficiency across the whole spectrum down to 0.633  $\mu\text{m}$ . With a small bias of 0.1 V, the external quantum efficiency (EQE) at 2.004  $\mu\text{m}$  improves to 54 %, as shown in Fig. 3(b).

The EQE is proportional to the photocurrent. With the 2.004  $\mu\text{m}$  wavelength light and our InAs diode, the photocurrent was made up of (1) minority holes in the  $n^+$  InAs layer that diffused to the depletion region,  $I_{diff,h}(V)$ , (2) drift and diffusion currents in the i-InAs layer, and (3) minority electrons in the  $p^+$  InAs layer that diffused to the

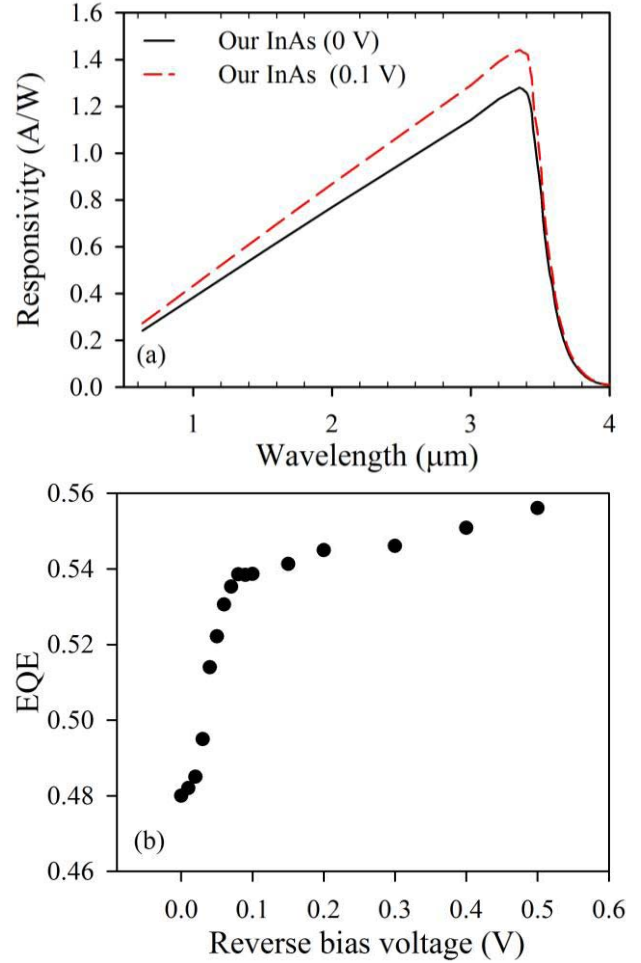


Fig. 3. (a) Room temperature responsivity as a function of wavelength. (b) External quantum efficiency (EQE) at a wavelength of 2.004  $\mu\text{m}$ .

depletion region. Contribution from (3) is negligible compared to (1) and (2) in this case since significant light absorption occurred in the top two layers. The bias dependence of  $I_{diff,h}(V)$  is described by [20]

$$I_{diff,h}(V) = \frac{qG_0}{\cosh(L(V)/L_d)},$$

where  $G_0$  is the generation rate of photocarriers in the illuminated surface,  $L(V)$  is the distance between the illuminated surface and depletion region edge (i.e the distance over which the holes must diffuse in order to contribute to  $I_{diff,h}$ ), and  $L_d$  is the minority carrier diffusion length. As reverse bias increases, the top depletion edge moves towards the device surface, reducing  $L$  and increases  $I_{diff,h}$  [20]. This effect applies also to the diffusion component in (2). Therefore we can expect increasing EQE with reverse bias, if the device indeed exhibits decreasing capacitance with reverse bias. This was confirmed for this work through capacitance-voltage measurements performed on devices at 77 K (cooling was used to reduce dark current, enabling accurate measurement). Using the capacitance value at 0 V we extracted an unintentional background doping of  $6 \times 10^{14} \text{ cm}^{-3}$  in the i-InAs layer of the  $p^+$ -i- $n^+$  diode, similar to the value achieved

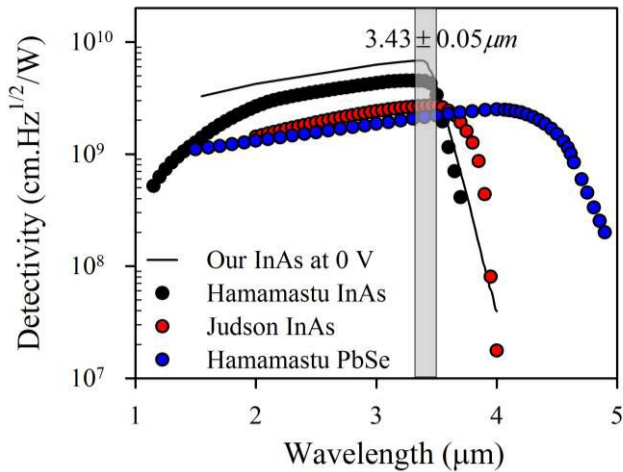


Fig. 4. Room temperature detectivity of our InAs diode, commercial InAs and PbSe detectors.

in reference [13]. Although the i-region was not fully depleted at 0 V, the unintentional background doping was significantly lower than the level of  $1\text{-}3 \times 10^{16} \text{ cm}^{-3}$  in the undoped InAs substrates [21]. This suggests that epitaxially grown InAs is required to maximize the depletion width and they could have advantages over InAs diodes fabricated via implantation on InAs substrates.

Using the measured responsivity and dark current, detectivity values were calculated for our InAs diodes and compared to those from commercial InAs diodes in Fig. 4. Our InAs photodiode has a higher peak detectivity at  $3.43 \mu\text{m}$ , than the InAs diodes from Judson [22] and Hamamatsu [23], suggesting the potential of epitaxially grown InAs. Our InAs diode also shows higher detectivity at the wavelength range defined by a  $3.43 \mu\text{m}$  filter.

It is tempting to increase the bias to achieve wider depletion width and hence higher responsivity. However increasing the bias also increases the dark current, as shown in Fig. 2. As the bias increased from 0 to 0.1 V, the device dark current increased by 10 times whereas the peak responsivity only improved by 13%. Therefore, radiation thermometry measurements were performed at 0 V, on our InAs photodiode, to minimize the detrimental effects of the device dark current.

To evaluate the performance of our InAs photodiode as a detector for radiation thermometry, we performed measurements using our InAs photodiode at room temperature. Fig. 5(a) and (b) shows the mean output photocurrent and SNR versus blackbody temperature, respectively. In this work, the blackbody source used had a lower temperature limit of  $50^\circ\text{C}$ . As expected, the output photocurrent and SNR increased with blackbody temperature. To investigate the potential of InAs for a  $3.43 \mu\text{m}$  radiation thermometer, we have also evaluated the performance of InAs when a  $3.43 \mu\text{m}$  narrow band filter was inserted into the setup in Fig. 1(b). The data obtained with the filter is also shown in Fig. 5. The output photocurrent increased with the blackbody temperature as in the previous set of measurements taken without the filter. Due to incomplete transmittance (76 %) and 62 nm FWHM

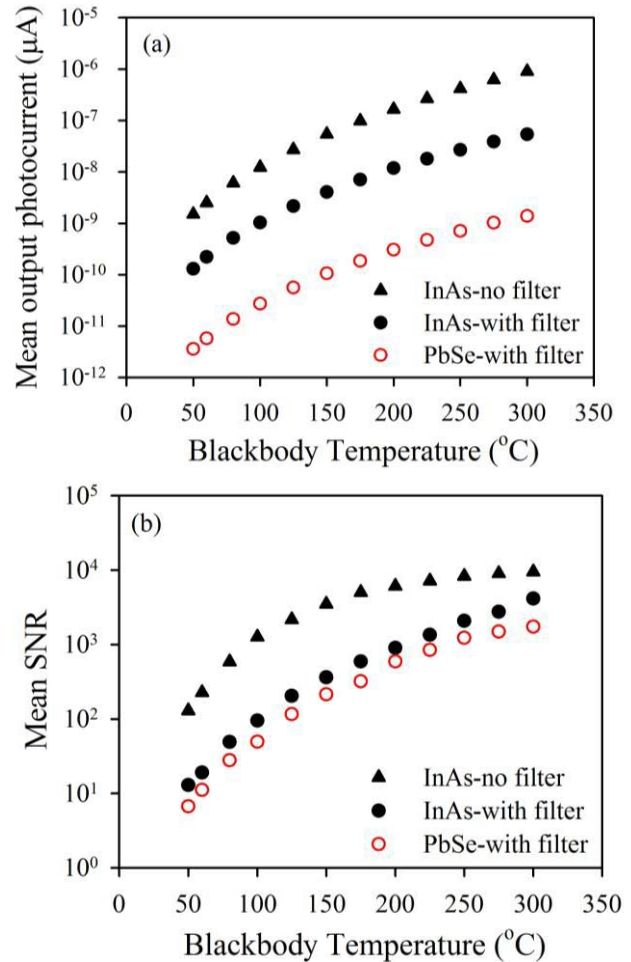


Fig. 5. (a) Mean photocurrent and (b) signal noise ratio of the InAs (closed symbols) at room temperature measured with and without a  $3.43 \mu\text{m}$  filter and PbSe (open symbols) measured with a  $3.43 \mu\text{m}$  filter.

bandwidth of the filter, the output photocurrent was reduced. However, the signal is still sufficiently strong for sensing object temperatures above  $50^\circ\text{C}$ .

As another candidate for a  $3.43 \mu\text{m}$  thermometer, the performance from a commercial P9696-03 PbSe photoconductor [24], which was reverse biased at 15 V and had a much larger active region area of  $9 \text{ mm}^2$ , was compared with our InAs. Our InAs diode produced higher output photocurrent than the commercial PbSe over the blackbody temperature range measured, as expected from the higher detectivity of InAs photodiodes than that of PbSe in Fig. 4. Due to its lower responsivity at  $3.43 \mu\text{m}$  wavelength, the PbSe photodiode achieved a lower SNR than that of our InAs diode, as shown in Fig. 5(b).

It is worth noting that the PbSe detector used in the radiation thermometry experiments was larger than InAs photodiode. The energy throughput in optical system is determined by the solid angle formed between the detector and the lens, which is given by  $A_1 \times A_2/D^2$  [25], where  $A_1$  and  $A_2$  are the lens and detector surface areas and  $D$  is the distance between two surfaces. The radiance flux incident upon  $A_2$  should equal to the flux leaving  $A_1$ . With a large active area, the PbSe has an illuminated area of 1.5 mm in diameter and can collect

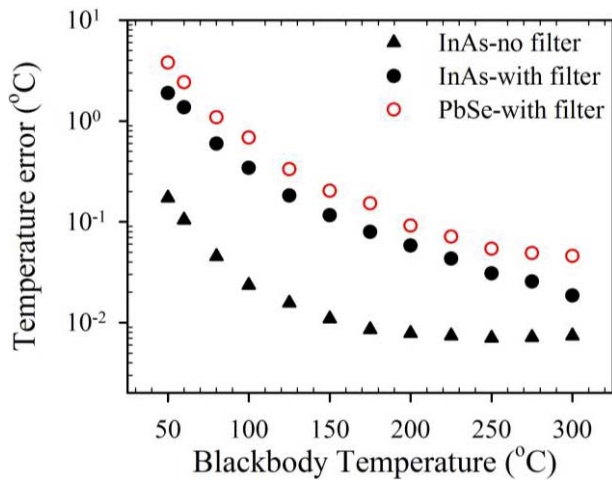


Fig. 6. Temperature error of the InAs detector (at 0 V) and the PbSe detector as a function of blackbody temperature.

all the energy from the optical system, corresponding to an optical power throughput factor of  $0.35 \text{ mm}^2\text{sr}$ . Our InAs only collected a small amount of the signal with an optical power throughput factor of  $0.016 \text{ mm}^2\text{sr}$ . Therefore, PbSe received 21.3 times of more energy than our InAs. Despite receiving less energy than PbSe, InAs still produced higher output photocurrent and SNR. This suggests that further improvement in the optical set up could increase the performance of InAs diode.

Fig. 6 shows the temperature errors of our InAs photodiode and the commercial PbSe photoconductor, as functions of blackbody source temperature. As the blackbody temperature increases, the temperature error reduces, due to increased SNR. Without the filter, the temperature error of InAs diode reduced from  $0.17 \text{ }^\circ\text{C}$  at  $50 \text{ }^\circ\text{C}$  to  $0.007 \text{ }^\circ\text{C}$  at  $300 \text{ }^\circ\text{C}$ . These measurement uncertainties are well within acceptable errors in radiation thermometry [26]. Clearly uncooled InAs photodiodes can accurately detect object temperatures of  $50 \text{ }^\circ\text{C}$  and higher. When the  $3.43 \text{ } \mu\text{m}$  filter is included, InAs still shows lower temperature error than PbSe, in spite of the reduced detected energy, across the entire temperature range. The reduced signal, however, increases the temperature error of the InAs thermometer to  $1.88 \text{ }^\circ\text{C}$  at  $50 \text{ }^\circ\text{C}$  and  $0.018 \text{ }^\circ\text{C}$  at  $300 \text{ }^\circ\text{C}$ . Assuming an acceptable temperature error of  $\pm 2 \text{ }^\circ\text{C}$  [26], InAs can be used for measuring temperature of  $50 \text{ }^\circ\text{C}$  or higher. These results confirm that InAs can outperform PbSe in applications requiring a  $3.43 \text{ } \mu\text{m}$  operating wavelength. For example, bi-axially oriented film extrusion and extrusion coating in plastics industry often works at high temperatures above  $200 \text{ }^\circ\text{C}$  [12]. In such applications, our InAs photodiodes will produce a temperature error of less than  $0.05 \text{ }^\circ\text{C}$  at  $200 \text{ }^\circ\text{C}$ .

#### IV. CONCLUSION

We have studied the performance of InAs photodiodes for use in radiation thermometry. The lowest temperature measured using our uncooled InAs photodiode is  $50 \text{ }^\circ\text{C}$  (limited by the blackbody source) with a temperature error of  $0.17 \text{ }^\circ\text{C}$ . Compared with commercial InAs and PbSe detectors,

our InAs showed higher detectivity at  $3.43 \text{ } \mu\text{m}$ . Using a narrow band filter we also demonstrated that the signal at the wavelength of  $3.43 \text{ } \mu\text{m}$  is sufficiently strong to achieve accurate temperature measurements using an InAs diode. Despite unoptimised signal coupling to our InAs diode, the temperature error of our InAs based  $3.43 \text{ } \mu\text{m}$  narrow band radiation thermometer is lower than that of a commercial PbSe detector.

#### ACKNOWLEDGMENT

The authors would like to thank the EPSRC National Centre for III-V Technologies, University of Sheffield, for wafer growth and access to fabrication facilities.

#### REFERENCES

- [1] J. Dixon, "Radiation thermometry," *J. Phys. E, Sci. Instrum.*, vol. 21, no. 5, pp. 425–436, May 1988. [Online]. Available: <http://iopscience.iop.org/0022-3735/21/5/001>
- [2] K. G. Kreider *et al.*, "Calibration of radiation thermometers in rapid thermal processing tools using Si wafers with thin-film thermocouples," in *Proc. AIP*, Chicago, IL, USA, 2002, pp. 1087–1092.
- [3] R. A. Holman, "Mold temperature measurement for glass-pressing processes," in *Proc. Symp. Appl. Radiat. Thermometry*, Philadelphia, PA, USA, 1985, pp. 67–73.
- [4] G. R. Peacock, "Ratio radiation thermometers in hot rolling and galvannealing of steel strip," in *Proc. AIP*, Chicago, IL, USA, 2003, pp. 789–794.
- [5] Z. M. Zhang, B. K. Tsai, and G. Machin, "Overview of radiation thermometry," in *Radiometric Temperature Measurements. I. Fundamentals*, vol. 42. San Diego, CA, USA: Academic, 2010, pp. 1–28.
- [6] T. J. Quinn, "Radiation thermometry," in *Temperature*. London, U.K.: Academic, 1990, pp. 332–431.
- [7] F. Sakuma and L. Ma, "Development of InGaAs radiation thermometers," in *Proc. SICE Annu. Conf.*, Tokyo, Japan, Aug. 2008, pp. 1614–1617.
- [8] Optris GmbH, Berlin, Germany. *Product Overview for Non-Contact Temperature Measurement*. [Online]. Available: <http://www.optris.co.uk/optris-gmbh>
- [9] Chino Corporation, Tokyo, Japan. (2012). *IR-CA Series High-Speed Compact Radiation Thermometers*. [Online]. Available: <http://www.chino.co.jp/english/products/thermometers/ir-ca.html>
- [10] V. Rudnev, D. Loveless, R. L. Cook, and M. Black, "Temperature measurement," in *Handbook of Induction Heating*. New York, NY, USA: Marcel Dekker, 2003, pp. 185–218.
- [11] Land Instruments International Ltd., Sheffield, U.K. (2012). *LSP-HD 71-Plastic & Thermoforming*. [Online]. Available: <http://www.landinst.com/products/lsp-hd-71-infrared-linescanner/documentation>
- [12] Z. M. Zhang, B. K. Tsai, and G. Machin, "Industrial applications of radiation thermometry," in *Radiometric Temperature Measurements: II. Applications*, vol. 43. San Diego, CA, USA: Academic, 2010, pp. 2–54.
- [13] P. J. Ker, A. R. J. Marshall, A. B. Krysa, J. P. R. David, and C. H. Tan, "Temperature dependence of leakage current in InAs avalanche photodiodes," *IEEE J. Quantum Electron.*, vol. 47, no. 8, pp. 1123–1128, Aug. 2011. Available: [http://ieeexplore.ieee.org/xpls/abs\\_all.jsp?arnumber=5871995&tag=1](http://ieeexplore.ieee.org/xpls/abs_all.jsp?arnumber=5871995&tag=1)
- [14] A. R. J. Marshall, C. H. Tan, M. J. Steer, and J. P. R. David, "Electron dominated impact ionization and avalanche gain characteristics in InAs photodiodes," *Appl. Phys. Lett.*, vol. 93, no. 11, p. 111107, Sep. 2008. [Online]. Available: <http://scitation.aip.org/content/aip/journal/apl/93/11/10.1063/1.2980451>
- [15] X. Zhou, M. J. Hobbs, B. S. White, J. P. R. David, J. R. Willmott, and C. H. Tan, "An InGaAlAs-InGaAs two-color photodetector for ratio thermometry," *IEEE Trans. Electron Devices*, vol. 61, no. 3, pp. 838–843, Mar. 2014. [Online]. Available: <http://ieeexplore.ieee.org/stamp/stamp.jsp?arnumber=6740070>
- [16] J. Taylor, *Foundation Level Infrared Training Notes—ISA*, Land Infrared Int. Ltd., Sheffield, U.K., Aug. 2010.
- [17] P. Saunders, "General interpolation equations for the calibration of radiation thermometers," *Metrologia*, vol. 34, no. 3, pp. 201–210, Jun. 1997. [Online]. Available: <http://iopscience.iop.org/0026-1394/34/3/1>

- [18] J. W. Hahn and C. Rhee, "Interpolation equation for the calibration of infrared pyrometers," *Metrologia*, vol. 31, no. 1, pp. 27–32, 1994. [Online]. Available: <http://iopscience.iop.org/0026-1394/31/1/005>
- [19] P. Saunders, "Uncertainty arising from the use of the mean effective wavelength in realizing ITS-90," in *Proc. AIP*, 2002, pp. 639–644.
- [20] M. H. Woods, W. C. Johnson, and M. A. Lampert, "Use of a Schottky barrier to measure impact ionization coefficients in semiconductors," *Solid-State Electron.*, vol. 16, no. 3, pp. 381–394, Mar. 1973.
- [21] Wafer Technology Ltd., Milton Keynes, U.K. (Oct. 2014), *Indium Arsenide Epitaxy Ready Polished Wafers*. [Online]. Available: [http://www.wafertech.co.uk/\\_downloads/Indium-Arsenide.pdf](http://www.wafertech.co.uk/_downloads/Indium-Arsenide.pdf)
- [22] Teledyne Judson Technologies, Montgomeryville, PA, USA. (Mar. 2003). *J12 Indium Arsenide Detectors*. [Online]. Available: [http://www.judsontechnologies.com/files/pdf/InAs\\_shortform\\_Mar2003.pdf](http://www.judsontechnologies.com/files/pdf/InAs_shortform_Mar2003.pdf)
- [23] Hamamatsu Photonics, Hamamatsu, Japan. (Mar. 2012). *InAs Photovoltaic Detectors P10090 Series*. [Online]. Available: [http://www.hamamatsu.com/resources/pdf/ssd/p10090-01\\_etc\\_kird1099e.pdf](http://www.hamamatsu.com/resources/pdf/ssd/p10090-01_etc_kird1099e.pdf)
- [24] Hamamatsu Photonics, Hamamatsu, Japan. (Jul. 2013). *PbSe Photoconductive Detectors P9696 Series*. [Online]. Available: [http://www.hamamatsu.com/resources/pdf/ssd/p9696-02\\_etc\\_kird1073e.pdf](http://www.hamamatsu.com/resources/pdf/ssd/p9696-02_etc_kird1073e.pdf)
- [25] R. U. Datla and A. C. Parr, "Introduction to radiometry" in *Optical Radiometry, Experimental Methods in the Physical Sciences*, vol. 41. Oxford, U.K.: Academic Press, 2005, pp. 1–34.
- [26] G. Machin and B. Chu, "High quality blackbody sources for infrared thermometry and thermography between  $-40$  °C and  $1000$  °C," *Imag. Sci.*, vol. 48, no. 1, pp. 15–22, 2000.

**Xinxin Zhou** received the M.Sc. and Ph.D. degrees in electronic engineering from the University of Sheffield, in 2010 and 2014, respectively.

She has been a Research Associate with the Electronic and Electrical Engineering Department, The University of Sheffield, since 2014. Her current research interests include fabrication and characterization of mid-infrared photodiodes, single-photon avalanche diodes and high-speed avalanche photodiodes, and simulations of avalanche photodiodes.

**Xiao Meng** received the B.Eng. degree from the Department of Electrical Engineering and Electronics, University of Liverpool, in 2011. He is currently pursuing the Ph.D. degree at the University of Sheffield, Sheffield, U.K.

His current research interests include single-photon avalanche diodes and X-ray detectors.

**Andrey B. Krysa** received the Degree from the Moscow Engineering Physics Institute, Moscow, Russia, in 1990, and the Ph.D. degree in solid-state physics from the Lebedev Physical Institute, Russian Academy of Sciences, Moscow, in 1997.

He joined the EPSRC National Centre for III–V Technologies, University of Sheffield, Sheffield, U.K., in 2001. Since then, he has been involved in the MOVPE of the Group III phosphides and arsenides.

**Jon R. Willmott** received the M.Phys. and Ph.D. degrees from the University of Southampton, Southampton, U.K., in 2003.

He was involved in optical engineering research at the University of Cambridge. He became a Physicist with Land Instruments International Ltd., Dronfield, U.K., in 2004. He has recently become a Senior Lecturer of Sensor Systems with the University of Sheffield, Sheffield, U.K., where he is an expert in radiation thermometry, thermal imaging, optical design, instrumentation, and radiometry.

**Jo Shien Ng** (M'99) received the B.Eng. and Ph.D. degrees in electrical and electronic engineering from the University of Sheffield, Sheffield, U.K., in 1999 and 2003, respectively.

She was with the university of Sheffield, from 2003 to 2006, and was responsible for characterization with the National Centre for III–V Technologies. She became a Royal Society University Research Fellow in 2006. Her research interests include avalanche photodiodes, Geiger-mode avalanche photodiodes, and material characterization.

**Chee Hing Tan** (M'95) received the B.Eng. and Ph.D. degrees in electronic engineering from the Department of Electronic and Electrical Engineering, University of Sheffield, Sheffield, U.K., in 1998 and 2002, respectively.

He is currently a Professor of Opto-Electronic Sensors with the Department of Electronic and Electrical Engineering, University of Sheffield. He has extensive experience in the characterization and modeling of high-speed low-noise avalanche photodiodes and phototransistors. His current research interests include single-photon avalanche diodes, mid-infrared photodiodes, quantum-dot infrared detectors, X-ray detectors, ultrahigh-speed avalanche photodiodes, and phototransistors.